Journal of the Brazilian Society of Mechanical Sciences and Engineering (2024) 46:184
https://doi.org/10.1007/s40430-024-04699-z

TECHNICAL PAPER

Adaptive cruise control system with fractional order ANFIS PD+I controller: optimization and validation

Prabhakar Gunasekaran[1] · Rajaram Sivasubramanian[1] · Karuppasamy Periyasamy[2] · Suresh Muthusamy[3] · Om Prava Mishra[4] · Ponarun Ramamoorthi[5] · Kishor Kumar Sadasivuni[6,7] · Mithra Geetha[6]

Received: 10 May 2023 / Accepted: 11 January 2024 / Published online: 7 March 2024

Abstract

Designing the control structures of fractional order PID controllers has proven to be effective in providing adaptability in set point tracing the performance of a nonlinear cruise control system. Wheel rolling resistance, wind drag force, and road gradient are incorporated into the design to better describe the system under consideration and to show how the nonlinear cruise control system behaves. This study presents a comparative investigation using simulation between control structures such as fractional order proportional–integral–derivative, fractional order integral minus proportional derivative, and fractional order proportional integral minus derivative. By preserving integral error indices as the goal function, a genetic algorithm is used to improve the controller gain parameters and fractional scaling values. To prevent integral windup conflicts and derivative boost issues, both traditional fractional order structures and adaptive neuro-fuzzy-based fractional order structures were used to create the adaptive cruise control system. The FO ANFIS PD plus I controller for the cruise control system exceeds the competition in servo and regulatory difficulties.

Keywords Wheel rolling resistance · Cruise control system · Fractional order structures · Genetic algorithm

Abbreviations

FOPID	Fractional order proportional–integral–derivative
FOI−PD	Fractional order integral minus proportional derivative
PI−D	Fractional order proportional integral minus derivative
ANFIS FO PD+I	ANFIS fractional order proportional derivative plus integral
ANFIS FOPID	ANFIS fractional order proportional–integral–derivative
ACC	Adaptive cruise control

Technical Editor: Rogério Sales Gonçalves.

✉ Ponarun Ramamoorthi
r.ponarun@gmail.com

Prabhakar Gunasekaran
gprabhakar2488@gmail.com

Karuppasamy Periyasamy
pkaruppasamy96@gmail.com

Suresh Muthusamy
infostosuresh@gmail.com

Kishor Kumar Sadasivuni
kishor_kumars@yahoo.com

[1] Department of Electronics and Communication Engineering, Thiagarajar College of Engineering (Government Aided and Autonomous), Madurai, Tamil Nadu, India

[2] Department of Electronics and Communication Engineering, Adhiyamaan College of Engineering (Autonomous), Hosur, Tamil Nadu, India

[3] Department of Electrical and Electronics Engineering, Kongu Engineering College (Autonomous), Perundurai, Tamil Nadu, India

[4] Department of Electronics and Communication Engineering, Vel Tech Rangarajan Dr, Sagunthala R&D Institute of Science and Technology, Chennai, Tamil Nadu, India

[5] Department of Electrical and Electronics Engineering, Theni Kammavar Sangam College of Technology, Theni, Tamil Nadu, India

[6] Centre for Advanced Materials, Qatar University, 2713 Doha, Qatar

[7] Department of Mechanical and Industrial Engineering, College of Engineering, Qatar University, 2713 Doha, Qatar

1 Introduction

The main intention of an adaptive cruise control (ACC) vehicle is to lessen the number of accidents by accomplishing greater deceleration or transitional maneuvers. To avoid or reduce the severity of a collision, the insecure reduction in speed should consider the technical constraints of the ACC system armed vehicles [1, 2]. While analyzing relevant research studies in the field of ACC systems, it is essential to comprehend the nature of the dynamic model and control [3] presented, as well as the effects generated by different sources on achieving an ACC system. The recent study has focused on how to onboard intelligent driver assistance technologies that may improve comfort and safety in urban areas and public road transportation networks [4].

The traditional PID control strategy is inappropriate for a complicated and nonlinear system. Much more emphasis is placed on fractional calculus in the discipline of control systems to fix nonlinearity in dynamic structures [5]. The fractional PID controller $PI^{\lambda}D^{\mu}$ has an integrator of order λ and a differentiator of order μ. It has been confirmed that this controller offers superior performance compared to the classical PID controller. FOPID controller is categorized by five factors: proportional gain, integration gain, derivative gain, integration order, and derivative order [6]. The two extra parameters give the controller designer more design options than a conventional PID controller but also make controller implementation more difficult. Regarding resilience, the controllers that use fractional order derivatives and integrals perform better than traditional controllers [7]. The fractional powers in integral and derivative relations are supplemented to obtain the FO controllers from the integer order [8]. The additional differential and integral order parameters boost the design flexibility of the controller, allowing for improved dynamic performance and durability when using this kind of controller. Compared to integer order systems, fractional order systems have exceptional performance [9]. To improve performance, the FOPID type controller has memory capability and can correctly change the controller's output based on error history data. Finally, the additional fractional order terms simplify modifying the closed high-frequency loop's and low-frequency properties [10].

FLC is also used with the fractional order controller to fine-tune parametric gains and optimum efficiency in the face of nonlinearities, load disturbances, and variations in plant parameters [11]. The fuzzy system's adaptive method will boost the fractional order controller's dynamic capability, enabling it to react quickly to stricture variations [12]. The genetic algorithm (GA) optimizes the scaling factors by minimizing many integral error indices while maintaining the control signal as the objective function [13]. A fractional order fuzzy PD+I controller (FOFPD+I) is designed and implemented to control complex, uncertain, and nonlinear robotic manipulators [14]. FOFPD+I controller has derived from fractional order PD and fractional order I controller. The proposed control strategy has an adaptive capability due to its nonlinear gains and preserves the linear structure of the fractional order PD+I controller [15].

A fractional order ANFIS PD plus I scheme is developed for improved control performance and quicker reaction times after taking these factors into account. This manuscript is organized as follows. In Sect. 2, the nonlinear system modeling is discussed. Section 3 demonstrates the design of the fractional order PID control structures. The strategy of FO ANFIS PID and FO ANFIS PD plus I structure is deliberated in Sect. 4. The adaptive neuro-fuzzy inference system for the cruise control system is portrayed in Sect. 5. Simulations of various controllers are merged as one plot for comparison in Sect. 6. Section 7 concludes the result discussions of the proposed research.

2 Nonlinear system modeling

The cruise control mechanism regulates the vehicle's speed by providing acceleration and deceleration signals to the engine control unit through the electronic control unit. This process generates a persistent velocity even in turbulences mainly instigated by alterations in the slope of a road. By considering the horizontal and slanting position of the car, the nonlinear example of the vehicle has been assembled based on Newton's law of motion [16] by incorporating parameters such as mass of the vehicle m, wind resistance B, wheel rolling resistance (Fr), and input force $cu(t)$ to the engine in both horizontal and slanting positions. It is shown in Fig. 1. The range of engine throttle varies from $0 \le u(t) \le 1$, and c represents the

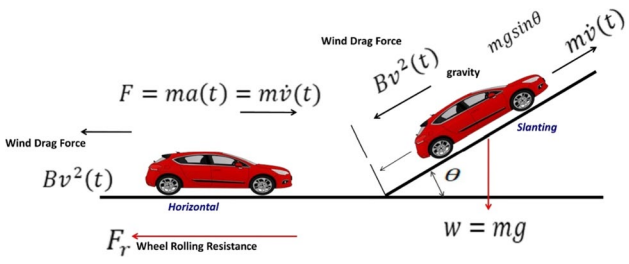

Fig. 1 Nonlinear system model

proportionality constant. Hence, the total force applied to the vehicle is $\mathrm{Ftot}(t) = ma(t) = m\dot{v}(t) = \mathrm{cu}(t), t \geq 0$.

Wind drag force acts as the first counterforce on the vehicle due to the product between wind resistance constant B and velocity squared time $v^2(t)$. The second counterforce emerged as wheel rolling resistance by combining the dimensionless rolling resistance coefficient C_r with mg. While considering the slanting position of the vehicle with an angle θ, road gradient force $mg\sin(\theta)$ has evolved as a third counterforce due to gravity. The angle considered for the slanting position is too small, representing it as $\sin\theta \approx \theta$.

$$F_r = C_\mathrm{r}W, \text{where } W = mg$$

$$F_r = C_\mathrm{r}mg$$

The equation of motion is now

$$m\dot{v} = \mathrm{cu}(t) - Bv^2(t) - C_\mathrm{r}mg - mg\sin\theta$$

$$\dot{v} = \frac{C}{m}u(t) - \frac{B}{m}v^2(t) - C_\mathrm{r}g - g\theta \tag{1}$$

The nature of Eq. (1) is nonlinear and differential, representing the velocity of the vehicle $v(t)$. Three significant scenarios are considered for linearization.

Scenario 1 Consider the car is on the flat plane ($\theta = 0$), and its desired regulated value is 1. Therefore, Eq. (1) is reformed as follows:

$$\dot{v} = \frac{C}{m}u(t) - \frac{B}{m}v^2(t) - C_\mathrm{r}g \tag{2}$$

$\dot{v}(t)$ becomes 0 when $t \to \infty$

Equation (2) is further reduced to

$$v_{\max}^2 = \frac{C}{B} - \frac{C_\mathrm{r}mg}{B}$$

$$v_{\max} = \sqrt{\frac{C}{B} - \frac{C_\mathrm{r}mg}{B}} = \sqrt{\frac{C - C_\mathrm{r}mg}{B}}$$

Scenario 2 While climbing the hill, the car will stall due to the full throttle applied to handle some crucial slanting angle θ_s and it, resulting in zero velocity. Therefore, the crucial slanting angle is expressed as follows:

$$0 = \frac{C}{m} - \frac{B}{m}(0) - C_\mathrm{r}g - g\sin\left(\theta_0\right)$$

$$\frac{C}{m} - C_\mathrm{r}g = g\sin\left(\theta_0\right)$$

$$\sin\left(\theta_0\right) = \frac{C - C_\mathrm{r}mg}{mg}$$

$$\theta_s = \theta_0 = sin^{-1}\left(\frac{C - C_rmg}{mg}\right)$$

This inspection is based on the assumption that the vehicle remains in a fixed gear. We most likely downshift to the lowest gear when driving a car to avoid stalling.

Scenario 3 Consider the car withextreme throttle and its slanting angle $\theta = 0$.

$$w = \frac{v}{v_{\max}} = \frac{v}{\sqrt{\frac{C - C_\mathrm{r}mg}{B}}},$$

where

$$v_{max} = \sqrt{\frac{C - C_rmg}{B}}$$

$$\frac{\mathrm{d}v(t)}{\mathrm{d}t} = \frac{C}{m}u(t) - \frac{B}{m}v^2(t) - C_\mathrm{r}g \tag{3}$$

where

$$v = w\sqrt{\frac{C - C_\mathrm{r}mg}{B}} \tag{4}$$

Differentiating Eq. (4) concerning t

$$\frac{\mathrm{d}v(t)}{\mathrm{d}t} = \frac{\mathrm{d}w}{\mathrm{d}t}\sqrt{\frac{C - C_\mathrm{r}mg}{B}}$$

Substitute in Eq. (3)

$$\frac{\mathrm{d}w(t)}{\mathrm{d}t}\sqrt{\frac{C - C_\mathrm{r}mg}{B}} = \frac{C}{m}u(t) - \frac{B}{m}\left(\frac{C - C_\mathrm{r}mg}{B}\right)w^2(t) - C_\mathrm{r}g$$

$$\frac{\mathrm{d}w(t)}{\mathrm{d}t} = \frac{C}{m}\sqrt{\frac{B}{C - C_\mathrm{r}mg}}u(t) - \frac{B}{m}\sqrt{\frac{C - C_\mathrm{r}mg}{B}}w^2(t) - C_\mathrm{r}g\sqrt{\frac{B}{C - C_\mathrm{r}mg}}$$

Assume $\alpha = \sqrt{\frac{C - C_\mathrm{r}mg}{B}}$

Henceforth, the nonlinear equation of the vehicle is

$$\frac{\mathrm{d}w(t)}{\mathrm{d}t} = \frac{C}{m}\frac{1}{\alpha}u(t) - \frac{B}{m}\alpha w^2(t) - \frac{C_\mathrm{r}g}{\alpha} \tag{5}$$

The meticulousresult of this streamlined form is $v(t) = v_{\max}\tanh(t\,\alpha)$. Figure 2 shows the Simulink model of the nonlinear equation, and its parameters are listed in Table 1.

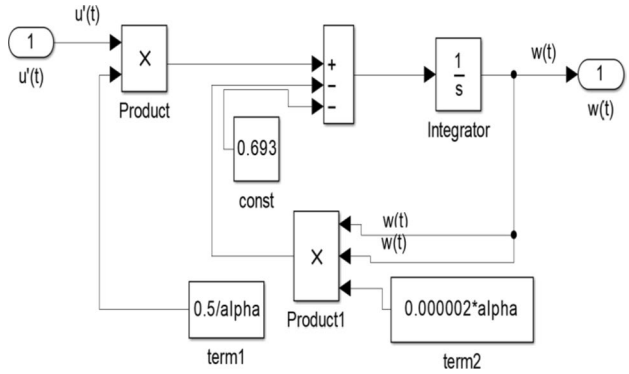

Fig. 2 Simulink model of the vehicle

Table 1 Design considerations

System features	Considerations
Mass of the car (m)	1250 kg
Air resistance (B)	2.5 Nsec/m
Proportionality constant (C)	6250 N
Engine supplied force (F)	C u(t), $t \geq 0$
Range of engine throttle	$0 \leq u(t) \leq 1$
Gravitational constant (g)	9.8 m/s^2
Rolling resistance coefficient (C_r)	0.495 (dimensionless)

3 Fractional order PID control structures

The derivatives and integrals of fractional calculus can be any real integer [7]. The FOPID PI$^{\lambda}D^{\mu}$ controller is a leeway of conventional PID controller [9], where a new integral factor λ and a new derivative factor μ have fractional values that augment more flexibility and make the system less subtle to factor changes. The differential equation of the parallel PI$^{\lambda}D^{\mu}$ controller can be defined as follows:

$$G_c^{\mathrm{FOPID}}(s) = k_{\mathrm{p}} + K_{\mathrm{i}}\frac{1}{s^{\lambda}} + k_{\mathrm{d}}s^{\mu} \tag{6}$$

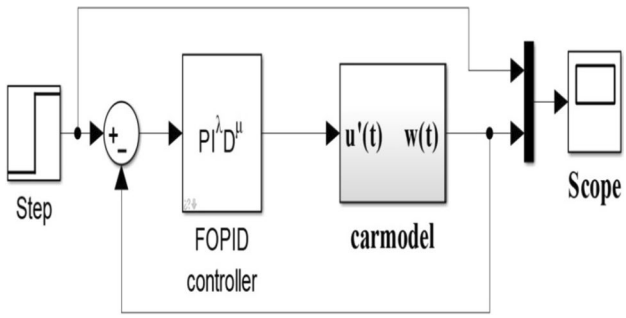

Fig. 3 Closed-loop model of the system with FOPID controller

where $k_{\mathrm{p}}, K_{\mathrm{i}}, k_{\mathrm{d}}$, λ, and μ are proportional gain, integral gain, derivative gain, and scaling factors. The ideals of these orders $\{\lambda, \mu\}$ along with $k_{\mathrm{p}}, K_{\mathrm{i}}, k_{\mathrm{d}}$ are the optimization variables in the genetic procedure. The FOMCON toolbox is used to advance the system controller based on Oustaloup's rational estimating approach [13]. Figure 4 represents the FOPID structure, while Fig. 3 depicts the closed-loop model of the system with an FOPID controller.

4 FO I–PD and FO PI–D controller

FOPI−D and FOI−PD structures have been introduced to reduce overshoot-damped oscillations and settling time. The fundamental goal of the redesigned structures is to shift the derivative component, the proportional component, or both from the critical route to the feedback path. Since the remaining terms will still transfer the change in set point, they are not directly affected by the jump in set value, but their impact on the comparable effect is still present. The construction of the fractional order PID controller is altered into a fractional order integral minus proportional derivative (FO I−PD) controller (Fig. 4).

$$uI^{\lambda} - \mathrm{PD}^{\mu}(t) = k_{\mathrm{I}}D^{-\lambda}e(t) - \left[k_{\mathrm{P}}y(t) + k_{\mathrm{D}}D^{\mu}y(t)\right] \tag{7}$$

where $uI^{\lambda} - \mathrm{PD}^{\mu}(t)$ is the control action of the fractional order I−PD controller.

The fractional order I−PD levers the unforeseen variations in the reference set point and eliminates the spikes from the control signal in the set point tracking approach. While in disturbance rejection mode, it fails to regulate the system smoothly due to the occurrence of spikes. To remove spikes from the response, the control structure is modified as a fractional order proportional integral minus derivative (PI−D) controller.

$$u\mathrm{PI}^{\lambda} - D^{\mu}(t) = \left[k_{\mathrm{P}}e(t) + k_{\mathrm{I}}D^{-\lambda}e(t)\right] - k_{\mathrm{D}}D^{\mu}y(t)] \tag{8}$$

where $u\mathrm{PI}^{\lambda} - D^{\mu}(t)$ is the control action of the fractional order PI−D. The structure of fractional order I−PD and fractional order PI−D is revealed in Figs. 5 and 6.

5 Design of FO ANFIS PID and FO ANFIS PD plus I structure

The fractional order adaptive neuro-fuzzy PID structureis framed by referring to various literature like fuzzy PID structure [14–17] with k_e and k_d. As the input scaling aspects and beta and alpha as output scaling aspects for better improvement, it is shown in Fig. 7. In this structure, the inputs to the fuzzy inference system are obtained by

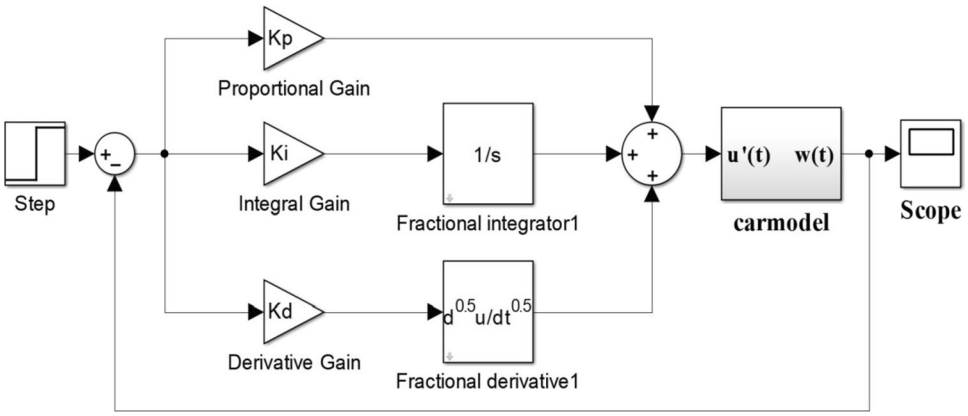

Fig. 4 FOPID structure

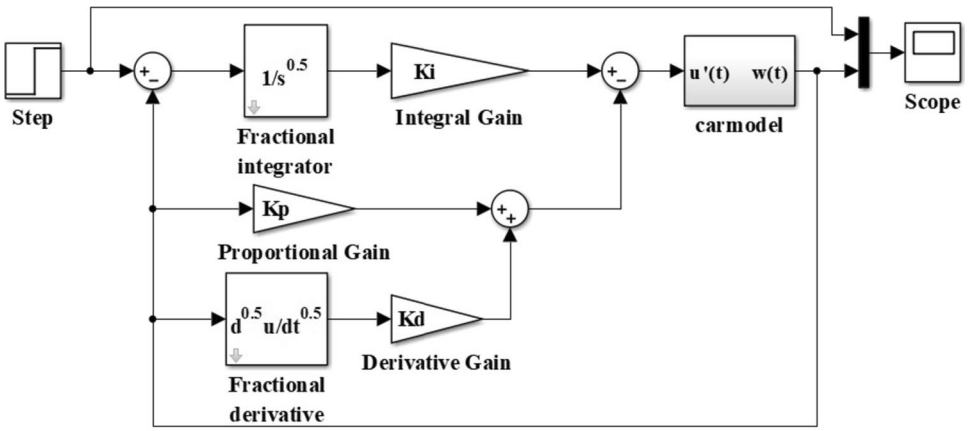

Fig. 5 FO I−PD controller

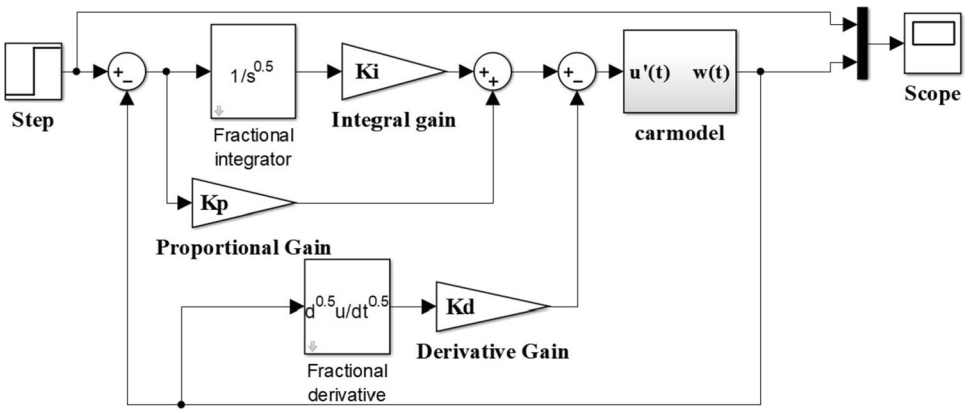

Fig. 6 FO PI−D controller

recording the model's error values and the derivative of error values. The output of the adaptive neuro-fuzzy was multiplied by alpha, and its integral was multiplied by beta before being added to form the total output of the controller. The integer order rate of the error at the ANFIS input is replaced with the fractional order counterpart (μ). At the ANFIS output, the order of the integral is likewise replaced with a fractional order (λ), denoting a fractional order integration of the ANFIS results. The ideals of these orders $\{\lambda, \mu\}$ along with k_e, k_{d} are the optimization variables in the genetic algorithm, and the alpha and beta values lie in the interval of $\{1, 2\}$ and $\{0, 1\}$, respectively, to accomplish the superior response. Fractional order ANFIS PD plus I controller offers a very modest design procedure for the cruise control problem. The structure of the controller is shown in Fig. 8. The inputs to the fuzzy inference system are obtained by recording the model's error values and derivative error values. Then, the derivative output is

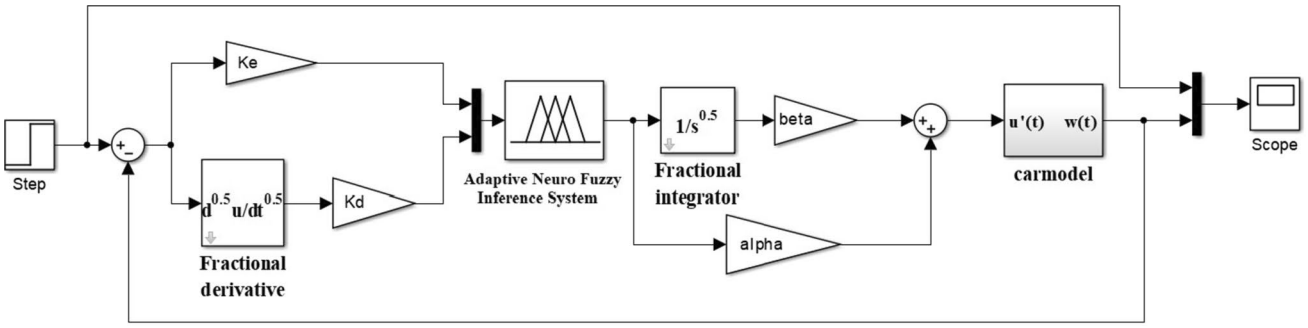

Fig. 7 FO ANFIS PID structure

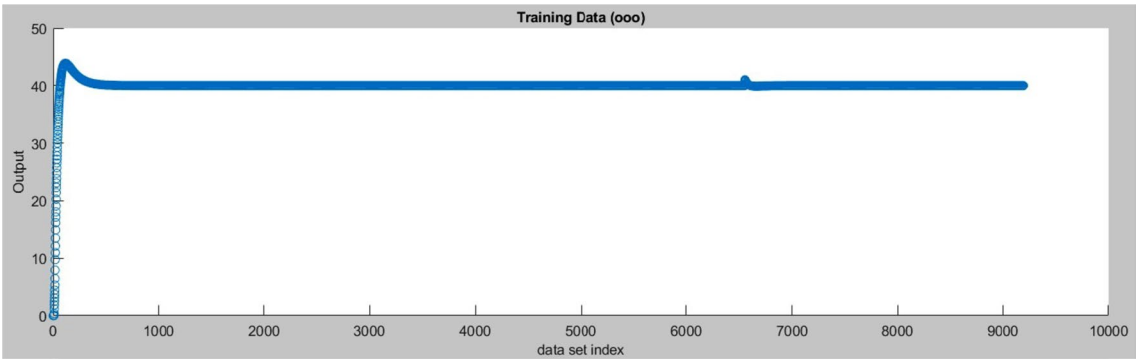

Fig. 8 ANFIS loading data

also provided to the ANFIS toolbox to avoid the problem of derivative kick. The Sugeno fuzzy system is reformed as the fuzzy inference system. An ANFIS with linguistic variables is articulated to pretend the control system. The Gaussian membership functions can define the linguistic ideals to solve nonlinearities which are uttered as follows:

$$\mu_{o_i}, h_i(x_i) = e^{\left[-\left(\frac{x_i - v_i.h_i}{\sigma_i.h_i}\right)\right]} \tag{9}$$

The output of the adaptive neuro-fuzzy inference system is then added to the output of the error integral. If a sustained error occurs in a steady state, integral action is required, which increases the control signal if there is a small positive error and decreases it when there is a negative error. To avoid the complexity of writing the rule base for the ANFIS PID controller and the problem of integral windup, incremental action is used in this control strategy instead of the integral of the error as an input to the fuzzy inference system. This incremental action augments a change in control signal Δu to the current control signal u,

$$ie_n = \sum_i (e_i * T_s)$$

where ie_n represents error at nth time instant, and T_s signifies sampling time.

The ANFIS uses the error with k_P and derivative error inputs with k_D for fractional order ANFIS PID and fractional order ANFIS PD plus I control structure to compute the scaling factor for proportional and derivative terms. Then, these ideals are used to appraise the gain aspects of fractional order ANFIS PID controller and fractional order ANFIS PD plus I controller. Hence, the final gain values of k_P, k_I, and k_D for FO ANFIS PID and FO ANFIS PD plus I controller are computed from the following expression:

$$k_P = k_P + \delta k_P$$

$$k_D = k_D + \delta k_D$$

$$k_I = k_I$$

These updated values are useful in framing the ANFIS FO PD plus I structure as follows:

$$\mathrm{PD}^{\mu}(t) + uI^{\lambda} = k_{\mathrm{P}}e(t) + k_{\mathrm{I}}D^{-\lambda}e(t) + k_{\mathrm{D}}D^{\mu}e(t) \tag{10}$$

Once the scaling factors are updated based on ANFIS, the fractional order ANFIS PD plus I controller will behave exactly as the linear PID controller.

6 Adaptive neuro-fuzzy inference system controller

ANFIS is artificial neural networks based on the Takagi–Sugeno fuzzy inference structure, which combines the quality of FLC [18–23] and neural networks. ANFIS is a Sugeno-type fuzzy inference scheme. The parameters connected with particular membership functions are computed utilizing either a back-propagation gradient descent algorithm alone or in grouping with the least squares technique. It has been broadly applied to unsystematic data sequences with extremely irregular dynamics. The range of error input is from −0.778 to 40, the error change is from −713.591 to 0.157, and the output range is from 9.675 to 10,000. Figures 9, 10, and 11 correspondingly represent the ANFIS loading data, trained data, and ANFIS structure. ANFIS parameters are listed in Table 2.

7 Optimal tuning

The parameters that organize the search space for the fractional order PID structures, including the adaptive neuro-fuzzy inference system, are $k_{\mathrm{p}}, k_{\mathrm{i}}, k_{\mathrm{d}}, \lambda$and μ. The intervals of the search space for these variables are $\{k_{\mathrm{p}}, k_{\mathrm{i}}, k_{\mathrm{d}}\} = [0, 600]$ and $\{\lambda, \mu\} = [0, 2]$. The variables are encrypted as real ideals in the procedure. The genetic algorithm has been widely used to find the best settings for controller tuning. To resolve the nonlinear model of the vehicle's cruise control system, the envisioned fractional order ANFIS PD plus I parameters are ideally adjusted using a genetic algorithm [24, 25]. Three distinct objective functions based on time-domain evaluation metrics have been created by incorporating the integral of squared control signal (ISCO) with diverse integral error indices such as IAE, ISE, and ITAE. It has been introduced by designing the proposed fractional order ANFIS PD plus I and its other versions such as fractional order ANFIS [26–28] PID,

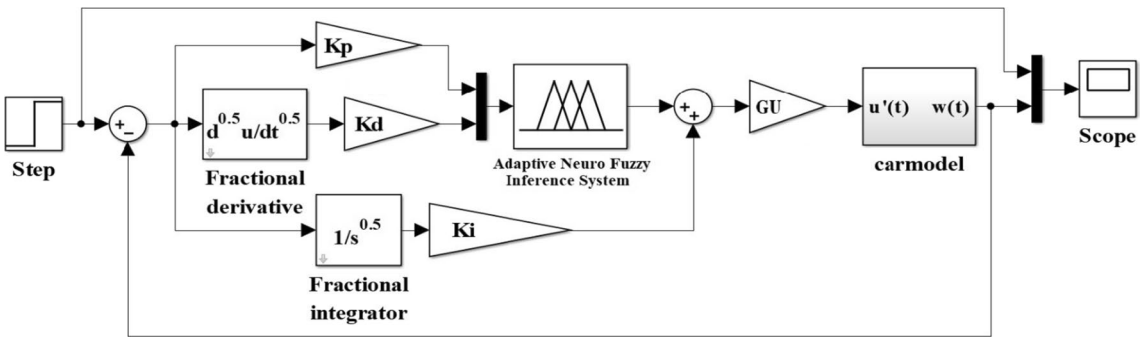

Fig. 9 FO ANFIS PD plus I structure

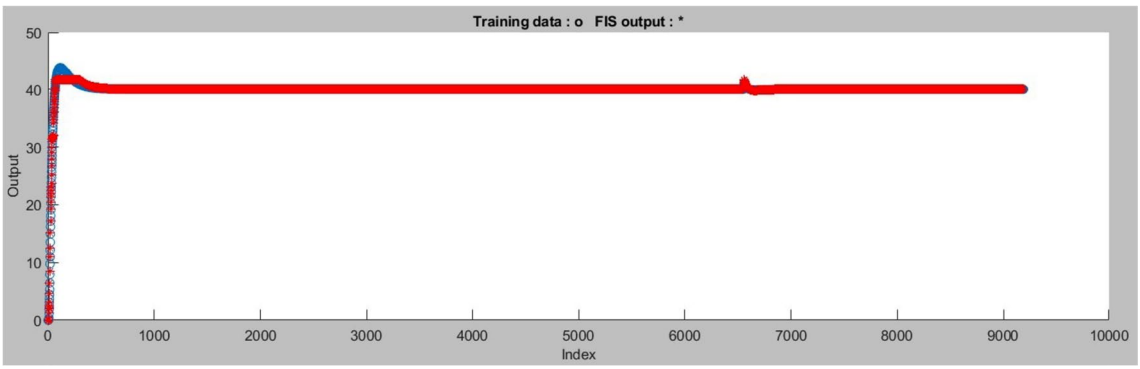

Fig. 10 Trained data and FIS output

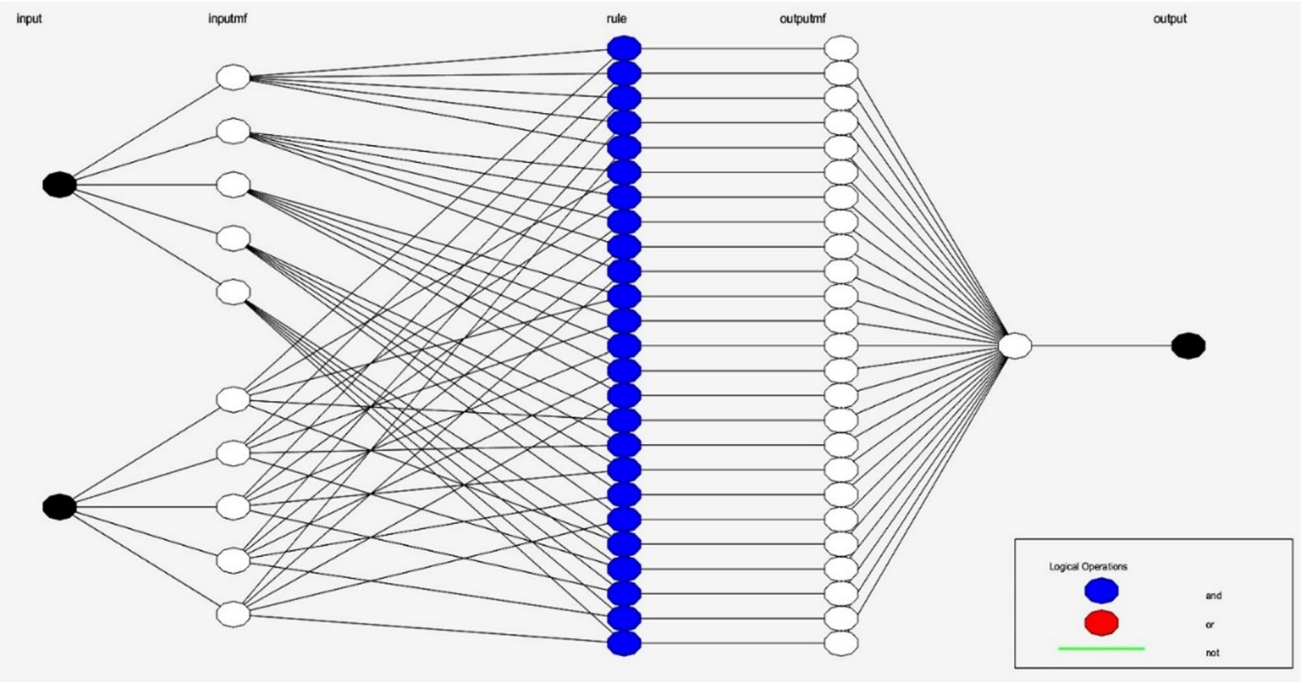

Fig. 11 ANFIS structure

Table 2 ANFIS parameters

Controller	ANFIS
Number of inputs	2
Membership functions type	GAUSSMF
Number of membership functions	5
Number of training data pairs	7378
Epoch number	6
Number of nodes	75
Number of linear parameters	25
Number of nonlinear parameters	20
Total number of parameters	45
Number of fuzzy rules	25
Error	0.837

FOPI−D, FOPID, and FOI−PD, sustaining the identical set of optimality norms. It is used to analyze the effort of the different controllers. Depending on the nature of the application and the relative importance of the error index and low control signal, the weights α in the control objective (11–13) allow the designer more options. To obtain controller parameters, optimization with equal factors loading for integral error indices and the integral control signal, i.e.,α is performed. Equations (11–13) show the three control objectives used in this simulation exercise.

$$O1 = \int_0^\infty \alpha|e(t)|\mathrm{d}t + \alpha u^2(t)\mathrm{d}t = (\alpha \times \text{ IAE}) + (\alpha \times \text{ ISCO}) \tag{11}$$

$$O2 = \int_0^\infty \alpha\left|e^2(t)\right|\mathrm{d}t + \alpha u^2(t)\mathrm{d}t = (\alpha \times \text{ISE}) + (\alpha \times \text{ISCO}) \tag{12}$$

$$O3 = \int_0^\infty \alpha(t|e(t)|)\mathrm{d}t + \alpha u^2(t)\mathrm{d}t = (\alpha \times \text{ITAE}) + (\alpha \times \text{ISCO}) \tag{13}$$

Over the rounds, GA gradually minimizes the objective functions (11–13) while determining the best custom settings for the fractional order fuzzy PID structure. The genetic algorithm pseudocode for controller parameter optimization is shown in Table 3. The population size is 250 to run the GA optimization algorithm associated with parameters such as normalized geometric selection, arithmetic crossover, and uniform mutation. This method terminates if the value of the desired function does not

Table 3 Pseudocode

Genetic Algorithm Pseudocode for Controller Parameter Optimization

```
# Define Constants and Hyperparameters
population size = 250
max_generations = 150
mutation_rate = 0.1
# Define Controller Types
controller_types = ["FO ANFIS PDplusI", "FO ANFIS PID", "FOPI-D", "FOPID", "FOI-PD"]
# Define Performance Indices
performance_indices = ["ISE+ISCO", "IAE+ISCO", "ITAE+ISCO"]
# Define Control Parameter Ranges and Initial Values for Each Controller Type
control_parameters = {
"FO ANFIS PDplusI": {"Kp/Ke": (0, 600), "Ki": (0, 600), "Kd": (0, 600), "λ": (0, 2), "μ": (0, 2)},
# Define similar parameter ranges and initial values for other controller types }
# Define Objective Function Evaluation function for Each Controller Type and Performance Index
def evaluate_objective_function(controller_type, performance_index, parameters):
# simulate the controller with the given parameters and compute the objective function value
# Return the calculated objective function value
# Main Genetic Algorithm Loop
for controller_type in controller_types:
    for performance_index in performance_indices:
        printf ("Optimizing {controller_type} under {performance_index}:")
        # Initialize the Population with Random Parameter Sets within Defined Ranges
        population = []
        for _ in range(population_size):
        random_parameters = generate_random_parameters (controller_type,
        control_parameters[controller_type])
        # Generate random parameters within defined ranges
        population.append(random_parameters)
        # Initialize variables to track the best solution
        best_parameters = None
        best_fitness = float('inf')
        # Genetic Algorithm Iterations
        for generation in range(max_generations):
        # Evaluate the Fitness of Each Individual in the Population
        fitness_scores = []
        for individuals in the population:
        fitness = evaluate_objective_function(controller_type, performance_index, individual)
        fitness_scores.append ((individual, fitness))
        # Sort the Population by Fitness (minimization)
        fitness_scores.sort(key=lambda x: x[1])
        # Select Parents for Crossover (e.g., using normalized geometric selection)
        parents = select_parents(fitness_scores)
```

significantly change between repetitions or if the maximum number of repetitions is reached. The number of repetitions is limited to 150. It is also significantly reduced as part of the goal function with GA to prevent massive control signals that could inundate the actuator and end up causing integral winding. Finally, curtailment of regulatory requirements (11–13) yields the optimal model for the fractional order ANFIS PD plus I and other controllers such as the FOPI−D, FOPID, and FOI−PD.

Table 3 (continued)

```
# create Offspring through Crossover (e.g., using arithmetic crossover)
offspring = []
while len(offspring) < population_size:
parent1, parent2 = select_two_parents(parents)
child = perform_crossover (parent1, parent2)
offspring.append(child)
# Apply Mutation (e.g., using uniform mutation)
for i in range(len(offspring)):
if random () < mutation_rate:
offspring[i] = mutate (offspring[i])
# Replace the Old Population with the New Offspring
population = offspring
# Update the best solution
if fitness_scores[0][1] < best_fitness:
best_parameters = fitness_scores[0][0]
best_fitness = fitness_scores[0][1]
# Print the optimized control parameters and objective function value
Printf("Optimal Parameters: {best_parameters}")
Printf("Minimum Objective Function Value: {best_fitness}")
```

Table 4 Optimal parameters of various controllers for servo response

Controller type	Performance index	Minimum value of the objective function	Control parameters				
			K_p/K_e	K_i	K_d	λ	μ
FO ANFIS PD plus I	ISE+ISCO	33.57	412.2	48.89	9.898	1.52	0.54
	IAE+ISCO	4.527					
	ITAE+ISCO	42.12					
FO ANFIS PID	ISE+ISCO	24.29	512.4	–	11.22	0.54	0.53
	IAE+ISCO	5.17					
	ITAE+ISCO	1082					
FOPI−D	ISE+ISCO	949.5	400	5	4	0.35	0.56
	IAE+ISCO	58.61					
	ITAE+ISCO	2392					
FOPID	ISE+ISCO	5066	432.23	58	10	1.5	0.6
	IAE+ISCO	283.3					
	ITAE+ISCO	4732					
FOI−PD	ISE+ISCO	15,030	200	6.34	5	0.34	0.5
	IAE+ISCO	663.7					
	ITAE+ISCO	5498					

8 Simulation results

The three objective functions (11–13) are minimized for each fractional order ANFIS PD plus I, fractional order ANFIS PID, FOPI-D, FOPID, and FOI−PD controller with the corresponding controller parameters described in Tables 4 and 5 for servo response and regulator response, respectively. By associating the outcomes in Tables 4 and 5, the objective function ($O1$) related to IAE provides the minimum value for all the controllers employed in this cruise control system, which signifies a great reduction in the controller effort. Therefore, the comparative investigation among the controllers has been made based on IAE-based tuning, displayed in Figs. 12 and 13. It reveals the cruise control system's servo and regulator behavior, respectively.

The servo response of FOPID shows large initial overshoot and damped oscillations with longer settling times but small spikes in the regulatory response. FOI−PD shows

Table 5 Optimal parameters of various controllers for regulator response

Controller type	Performance index	Minimum value of the objective function	Control parameters				
			K_p/K_e	K_i	K_d	λ	μ
FO ANFIS PD plus I	ISE+ISCO	33.57	412.2	48.89	9.898	1.52	0.54
	IAE+ISCO	4.527					
	ITAE+ISCO	42.12					
FO ANFIS PID	ISE+ISCO	24.29	512.4	–	11.22	0.54	0.53
	IAE+ISCO	5.17					
	ITAE+ISCO	1082					
FOPI−D	ISE+ISCO	949.5	400	5	4	0.35	0.56
	IAE+ISCO	58.61					
	ITAE+ISCO	2392					
FOPID	ISE+ISCO	5066	432.23	58	10	1.5	0.6
	IAE+ISCO	283.3					
	ITAE+ISCO	4732					
FOI−PD	ISE+ISCO	15,030	200	6.34	5	0.34	0.5
	IAE+ISCO	663.7					
	ITAE+ISCO	5498					

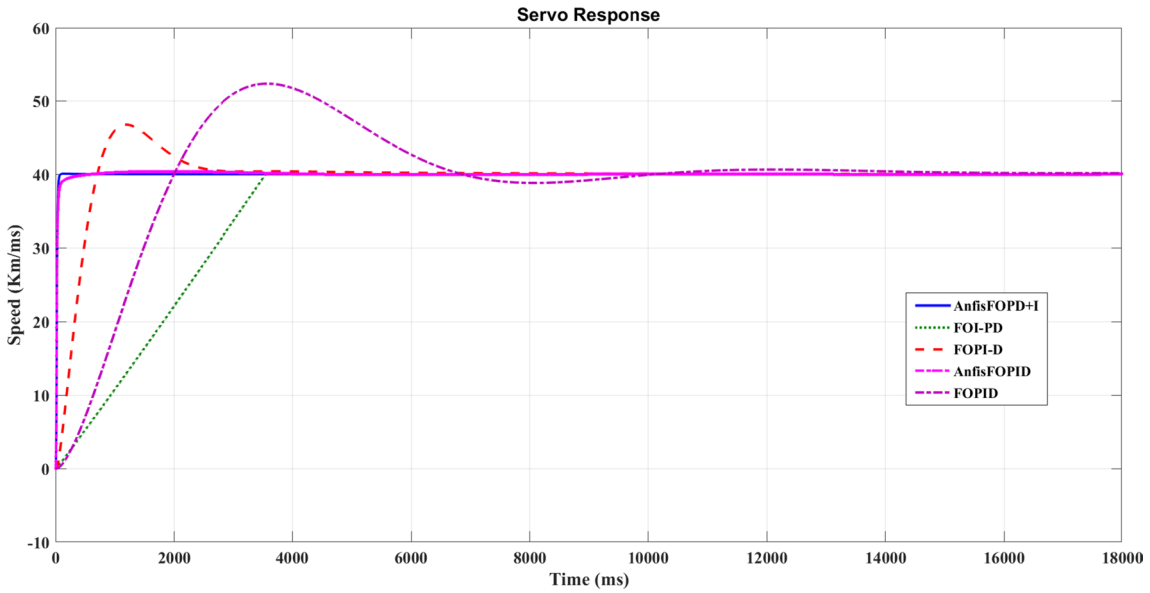

Fig. 12 Servo response for IAE-based tuning of different controllers

some delay in settling time with no overshoot in the servo response but a large enough spike in the regulatory response.

The servo response of FOPI−D has a little overshoot compared to FOPID and a little spike in the regulator response compared to FOI−PD. The set point tracking capability of FO ANFIS PD+I and FO ANFIS PID controllers is superior to non-ANFIS controllers such as FOPI−D, FOPID, and FOI−PD. Both the FO ANFIS PD plus I and the FO ANFIS PID contribute a lower peak overshoot and a better load turbulence response. Furthermore, the load turbulence behavior of the FOPI−D, FOPID, and FOI−PD controllers is limited. Hence, the FO ANFIS PD plus I confirms a noble load disturbance

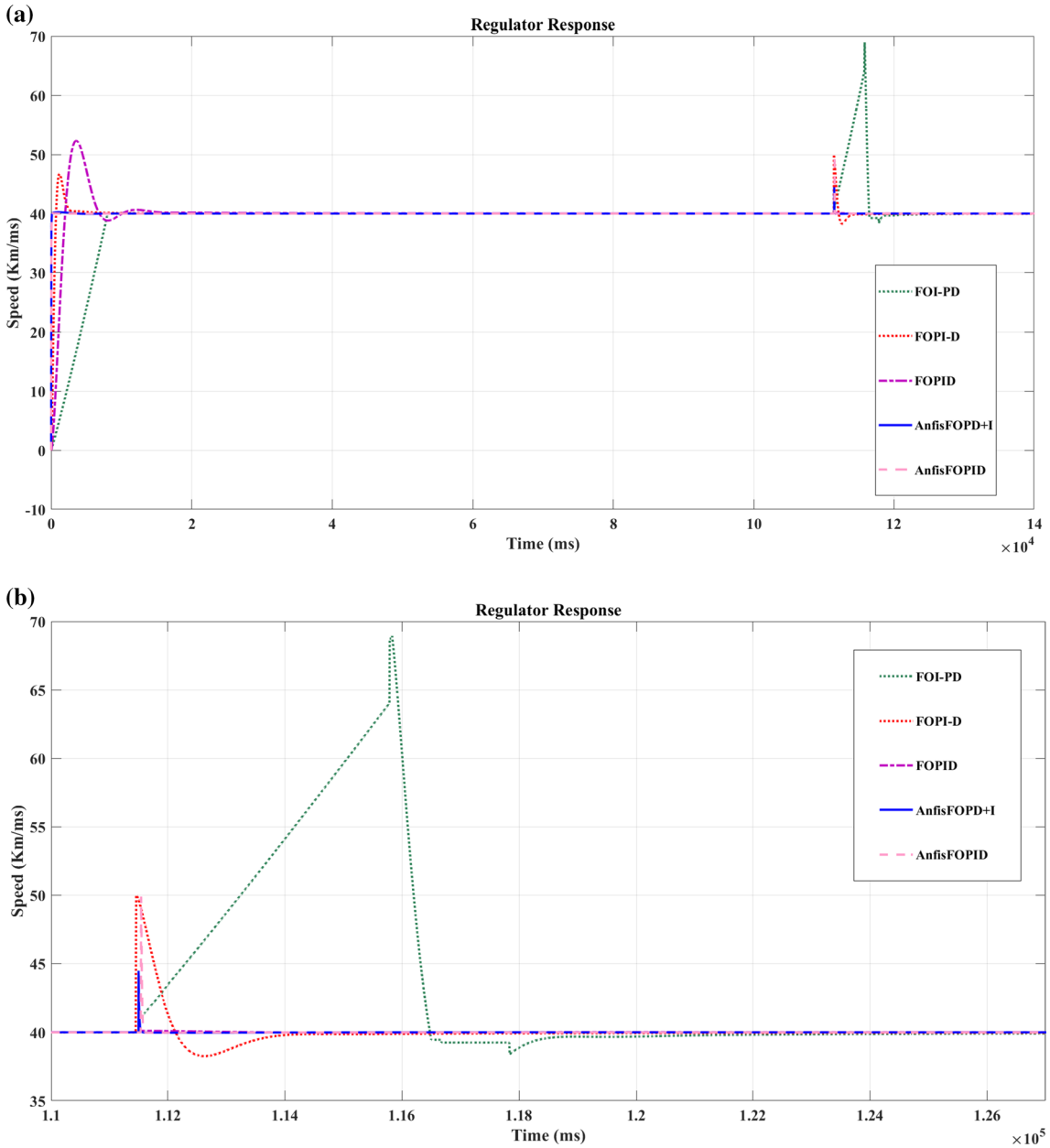

Fig. 13 **a** Regulator response for IAE-based tuning of different controllers and **b** close vision of regulator response

rejection and good set point tracking among all the controllers employed in the modeled cruise control system.

9 Conclusions

Therefore, this work carried out a successive investigation of fractional order controllers on cruise control systems by designing various control structures such as fractional order proportional–integral–derivative (FOPID), fractional order integral minus proportional derivative (FOI−PD), fractional order proportional integral minus derivative (FOPI-D), and adaptive neuro-fuzzy-based fractional order structures (FO ANFIS PID and FO ANFIS PD plus I). A genetic algorithm-based appropriate time-domain modification minimizes the linear combination of many integral evaluation metrics and the control signal. It is tuned for both servo and regulator responses to achieve optimal results. Adaptive

neuro-fuzzy-based fractional order structures are implemented to avoid integral windup and derivative kick issues. The performance of the controllers is seen to be impacted by the type of process to be regulated as well as the selection of integral evaluation metrics. Therefore, the performance of FO ANFIS PD plus I controller surpasses the others in set point tracing and load turbulence denial criteria based on the result comparison.

Author contributions All the authors have equally contributed to the work.

Funding Open Access funding provided by the Qatar National Library. This work was supported by the Qatar National Research Fund under Grant No. MME03-1226–210042. The statements made herein are solely the responsibility of the authors.

Data availability The data used to support the findings of this study are available from the corresponding author upon request.

Code availability The relevant code for the work is available with the authors.

Declarations

Conflict of interest The authors declared that they have no conflicts of interest in this work. We declare that we do not have any commercial or associative interest that represents a conflict of interest in connection with the work submitted.

References

1. Singh B, Bhattacharya A (2020) Review on safety problems with adaptive cruise control systems in automobiles. J Crit Rev 7(1):674–678
2. Wu C, Xu Z, Liu Y, Fu C, Li K, Hu M (2020) Spacing policies for adaptive cruise control: a survey. IEEE Access 8:50149–50162
3. Schakel WJ, Gorter CM, de Winter JCF, Van Arem B (2017) Driving characteristics and adaptive cruise control? A naturalistic driving study. IEEE Intell Transp Syst Mag 9(2):17–24
4. Hu C, Wang J (2021) Trust-based and individualizable adaptive cruise control using control barrier function approach with prescribed performance. IEEE Trans Intell Transp Syst 23(7):6974–6984
5. Gao B, Cai K, Qu T, Hu Y, Chen H (2020) Personalized adaptive cruise control based on online driving style recognition technology and model predictive control. IEEE Trans Veh Technol 69(11):12482–12496
6. Safaei M, Tavakoli S (2020) Improved PID tuning rules using fractional calculus. In: 28th Iranian conference on electrical engineering (ICEE), pp 1–5
7. Podlubny I (1999) Fractional-order systems and PI/sup /spl lambda//D/sup /spl mu//-controllers. IEEE Trans Autom Control 44(1):208–214
8. Chen Z, Yuan X, Ji B, Wang P, Tian H (2014) Design of a fractional order PID controller for hydraulic turbine regulating system using chaotic non-dominated sorting genetic algorithm II. Energy Convers Manage 84:390–404
9. Marzaki MH, Rahiman MHF, Adnan R, Tajjudin M (2015) Real-time performance comparison between PID and Fractional order PID controller in SMISD plant. In: IEEE 6th control and system graduate research colloquium (ICSGRC), pp 141–145
10. Muresan CI, Birs I, De Keyser R (2021) An alternative design approach for fractional order internal model controllers for time delay systems. J Adv Res 31:177–189
11. Oustaloup A, Levron F, Mathieu B, Nanot FM (2000) Frequency-band complex noninteger differentiator: characterization and synthesis. IEEE Trans Circuits Syst I: Fundam Theory Appl 47(1):25–39
12. Bruzzone L, Mario B, Pietro F (2021) Fractional-order $PII^{1/2}DD^{1/2}$ control: theoretical aspects and application to a mechatronic axis. Appl Sci 11(8):3631
13. Al-Dhaifallah M, Kanagaraj N, Nisar KS (2018) Fuzzy fractional-order PID controller for fractional model of pneumatic pressure system. Math Probl Eng 2018(1):1–9
14. Rebai A, Guesmi K, Hemici B (2015) Design of an optimized fractional order fuzzy PID controller for a piezoelectric actuator. Control Eng Appl Inf 17(3):41–49
15. Saptarshi D, Indranil P, Shantanu D, Amitava G (2012) A novel fractional order fuzzy PID controller and its optimal time domain tuning based on integral performance indices. Eng Appl Artif Intell 25(2):430–442
16. Chhabra H, Mohan V, Rani A et al (2020) Robust nonlinear fractional order fuzzy PD plus fuzzy I controller applied to the robotic manipulator. Neural Comput Appl 2020(7):2055–2079
17. M'Sirdi N, Abdelhamid R, Naamane A (2018) A nominal model for vehicle dynamics and estimation of input forces and tire friction. CSC 2007, Marrakech, Morocco. HAL-0196664.1
18. Baleanu D, Agarwal RP (2021) Fractional calculus in the sky. Adv Differ Equ. https://doi.org/10.1186/s13662-021-03270-7
19. Das S, Pan I, Das S, Gupta A (2012) A novel fractional order fuzzy PID controller and its optimal time domain tuning based on integral performance indices. Eng Appl Artif Intell 25(2):430–442
20. Tepljakov A, Petlenkov E, Belikov J (2011) FOMCON: fractional-order modeling and control toolbox for MATLAB. In: proceedings 18th international mixed design of integrated circuits and systems (MIXDES) conference, pp 684–689
21. Umamaheswari K, Prabhakar G, Viji K, Thanapal P (2021) ANFIS PD Plus I control on simscape model of nonlinear physical system. Control Eng Appl Inf 23(1):50–59
22. Liu F, Wang H, Shi Q, Wang H, Zhang M, Zhao H (2017) Comparison of an ANFIS and Fuzzy PID control model for

performance in a two-axis inertial stabilized platform. IEEE Access 5:12951–12962
23. Gunasekaran P, Sundaramoorthy S, Pulikesi NP (2019) Fault data injection attack on car-following model and mitigation based on interval type-2 fuzzy logic controller. IET Cyber-Phys Syst: Theory Appl 4:128–138
24. Nassef AM, Abdelkareem MA, Maghrabie HM, Baroutaji A (2023) Metaheuristic-based algorithms for optimizing fractional-order controllers—a recent, systematic, and comprehensive review. Fractal Fract. 7(7):553
25. Jayachitra A, Vinodha R (2014) Genetic algorithm based PID controller tuning approach for continuous stirred tank reactor. Adv Artif Intell 2014(791230):1–8
26. Kanagaraj N (2023) An adaptive neuro-fuzzy inference system to improve fractional order controller performance. Intell Autom Soft Comput 35(3):3213–3226
27. Saadat SA et al (2021) Adaptive neuro-fuzzy inference systems (ANFIS) controller design on a single-phase full-bridge inverter with a cascade fractional-order PID voltage controller. IET Power Electron 14:1960–1972
28. Ewees AA, Elaziz MA (2020) Improved adaptive neuro-fuzzy inference system using gray wolf optimization: a case study in predicting biochar yield. J Intell Syst 29(1):924–940